A Solution Processed Amorphous InGaZnO Thin-Film Transistor-Based Dosimeter for Gamma-Ray Detection and Its Reliability

Maruti B. Zalte, Virendra Kumar, Sandeep G. Surya, *Member, IEEE*, and Maryam Shojaei Baghini, *Senior Member, IEEE*

***Abstract*—Metal oxide semiconductors proved their usability in environmental monitoring applications and are considered successful in detecting ionizing radiation. This work reports the feasibility of solution-processed metal oxide semiconductor thin-film transistors for radiation sensing for the first time. In particular, the effects of a wide range of gamma radiation (100Gy to 10kGy) on the performance of solution-processed amorphous Indium-Gallium-Zinc-Oxide (a-IGZO) transistors are investigated. The current-voltage (IV) characterization (both output and transfer characteristics) of IGZO-TFTs before and after irradiation are obtained to study different parameters. The radiation-induced changes in TFT are mainly observed in the threshold voltage shift (ΔV_{th}) and the increase of subthreshold swing. It is observed that up to a total dose of 1kGy, threshold voltage increases negatively ($\Delta V_{th} = -1.8$V at 1 kGy), and beyond 1 kGy, threshold voltage increases positively ($\Delta V_{th} = 0.8$V at 10 kGy). The XRD and AFM data of IGZO thin-film suggests minor structural and morphological changes after exposure to gamma irradiation. The corresponding sensitivity obtained with gamma irradiation is 27.78 mV/Gy (100Gy-1kGy), expressed in the threshold voltage shift. The effects of radiation-induced changes in TFTs are completely removed after storing irradiated TFTs in the vacuum at room temperature for 6 months.**

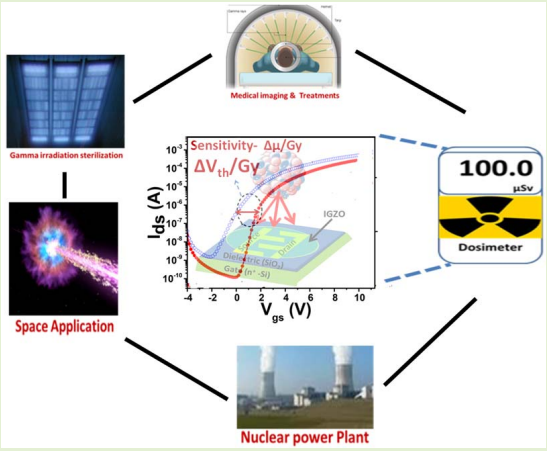

***Index Terms*—Thin-film, Gamma radiation, solution-process, sensor, transistor.**

I. Introduction

THE recent years have seen significant research on electronically functional materials that can be processed on large areas of the flexible and low-cost substrates. The materials, such as organic polymers, nanostructured materials, and amorphous oxides (AOs) have been explored to develop a range of novel applications such as light-emitting diodes, thin-film transistors, and sensors onto large-area surfaces [1]–[3]. Such devices' exposure to mechanical, photonic, or chemical stress must not disturb their electronic performance. Hence, the encapsulating materials are introduced in the device architecture to minimize the sensitive active layer's exposure to external chemicals or light and reduce mechanical stress [4]. However, the encapsulation strategy does not apply to protect the devices and their electronic performance in the harsh radiation environment as encountered in space, nuclear power plants, or medical diagnostics [5], [6]. To realize low-cost detectors or sensors without heavy metallic shielding, electronic materials can be processed at low cost and withstand the continuous exposure to high energy particles (α, protons, electrons) must be explored. The radiation hardness of traditional materials and devices related to complementary metal-oxide Semiconductors (CMOS) based electronics have been reported [5]. The amount of trapped charge in the dielectric tends to increase with the total ionizing dose. The trapped charge leads to space charge fields, causing threshold voltage shift and excessive leakage in CMOS structures. Also, the interfacial trap states created as a function of radiation dose at the SiO_2/ Si interface, act as scattering centers to the

Manuscript received January 25, 2021; revised February 21, 2021; accepted February 21, 2021. Date of publication February 24, 2021; date of current version April 5, 2021. This work was supported by the Department of Science and Technology (DST), Government of India for project under Grant SR/NM/TP-56/2016-IITB(G). The associate editor coordinating the review of this article and approving it for publication was Prof. Hsin-Ying Lee. *(Corresponding author: Maruti B. Zalte.)*

Maruti B. Zalte, Sandeep G. Surya, and Maryam Shojaei Baghini are with the Department of Electrical Engineering, Indian Institute of Technology Bombay, Mumbai 400076, India (e-mail: marutizalte@iitb.ac.in; sandeep.surya@hotmail.com; mshojaei@ee.iitb.ac.in).

Virendra Kumar is with the Radiation Technology Development Division, Bhabha Atomic Research Center (BARC), Mumbai 400085, India (e-mail: vkumar@barc.gov.in).

Digital Object Identifier 10.1109/JSEN.2021.3061955

nearby accumulation layer and deteriorate subthreshold slope and mobility [7]–[9]. Meanwhile, a CMOS compatible organic transistor was built and used in gamma radiation sensing, where authors reported reduced mobility and enhanced subthreshold swings upon increasing the dose (0 Gy to 3 Gy) [10]. However, the drawback of the sensor is its organic channel layer that deteriorates over time. Hence, the standard CMOS integrated circuit components show failure at a total dose less than 100 Gy. Previously, dedicated processing technology has been reported [11] that uses the reduced thickness of oxide dielectrics for preparing radiation-hard CMOS components. They withstand a dose level of 1 kGy (Si), as necessary for space applications [11], [12]. Polycrystalline silicon thin-film transistors (TFTs) fabricated using low-pressure chemical vapor deposition (LPCVD) exposed to γ-irradiation up to 10 kGy was found to be more susceptible to leakage current degradation leading to permanent failure of the devices [13]. The amorphous silicon TFTs fabricated on a flexible substrate show an increased subthreshold swing of 2V/decade and threshold voltage shifts of -2.1 V after an irradiation dose of 6.6 kGy [14].

Alternative material platforms for large-area electronic devices are transparent conducting oxides (TCO). The TCOs already find commercial applications in flat-panel displays, light-emitting diodes, solar cells and optoelectronic devices because of their outstanding electronic transport properties, optical transparency and easy and cheap processing. The possibility modifying physical properties by controlling stoichiometry of TCOs makes them suitable in the development of piezo-MEMS technology and ferromagnetic tunnel junctions [15].The TCOs are considered intrinsically stable semiconducting materials due to the high formation energy of the oxide-based ionic lattice and their amorphous structure. The amorphous-Indium Gallium Zinc Oxide (a-IGZO), which is also TCOs, has been used extensively as a channel material of TFTs in the last decade. The a-IGZO-TFT is a potential candidate to replace organic and amorphous silicon TFTs for driving active-matrix liquid crystal displays (AMLCDs) and active-matrix organic light-emitting diodes (AMOLEDs) because of their high field-effect mobility ($\sim$10 $cm^2.V^{-1}.s^{-1}$), good uniformity, and simple processing methods [16], [17]. The proper selection of concentration of Indium, Gallium and Zinc in the IGZO films ensures the TFTs with excellent electrical properties and stability [18]. The electrical conductivity in zinc oxide is controlled by zinc interstitials and/or oxygen vacancies so the optimization of zinc concentration is important. The high-k gate dielectric such as aluminium titanium oxide is reported to be better that ensure a pure amorphous film as compared to SiO2 and SiNx dielectrics [19]. Furthermore, solution-based processes of a-IGZO, such as spin-coating and inkjet printing, enable low cost, low temperature ($< 350°C$), and high throughput fabrication possibility on low-cost, flexible substrates without a need for vacuum facilities [20], [21].

The γ-irradiation effects on amorphous and polycrystalline TFTs fabricated using HMSOs such as polycrystalline-ZnO (poly-ZnO), amorphous-IZO (a-IZO), and crystalline-IGZO (C-IGZO) are investigated. The poly-ZnO TFTs fabricated using vacuum processing and with Al_2O_3 dielectric exhibited good stability toward γ-irradiation dose of 1MGy with a threshold voltage (ΔV_{th}) shift of -1.8 V and nearly constant field-effect mobility [22]. Amorphous IZO-TFTs with SiO_2 gate dielectric exposed to the γ-irradiation dose of 3 kGy had performance degradations, including a sub-threshold swing rise of 250mV/decade and V_{th} shifts of around -10V [23]. Another study on a-IZO–TFTs exposed to irradiation of 15 kGy reported V_{th} shifts of around -15V and severe device degradations [24]. The crystalline IGZO-TFTs exposed to $^{12}C^{6+}$ beam heavy ion irradiation exhibited good stability with V_{th} shifts of 1V and subthreshold swing of 250mV/decade after 1.3 kGy exposure [25]. As reported, Gallium creates a stronger bond with oxygen than Indium or Zinc that ensures better stability in amorphous a-IGZO-TFTs than in a-IZO-TFTs. The merits, such as strong ionic bonding of the metal oxide-based semiconductor channel, fabrication on the low cost flexible substrates without the need of vacuum processes, and the low power consumption due to the controlled off-state leakage current can make a-IGZO-TFTs suitable for applications in harsh radiation environments such as spacecraft, nuclear reactors, medical radiation detectors, and high-energy particle accelerators [26], [27].

To the best of our knowledge, no work has been reported on the effects of γ-irradiation on n-channel enhancement-mode solution-processed a-IGZO TFT. In this work, the electrical characteristics of solution-processed a-IGZO TFTs are presented before and after gamma irradiation to high-total-dose levels. The corresponding device parameters have been segregated into two exposure regimes, to signify the effects of irradiation and to diversify applications. The effects of ionizing radiations on the effective channel mobility, radiation-induced traps, threshold voltage shift, and response to room temperature annealing are investigated.

The sensitivities extracted are of 0.13×10^{-3} $cm^2.V^{-1}.s^{-1}$/Gy and 27.78 mV/Gy for mobility and threshold voltage, respectively. Further, the proposed γ-radiation sensor stored in a vacuum ambiance showed complete recovery, ensuring its reusability.

II. Synthesis, Fabrication & Characterization

A. Synthesis of IGZO Solution

The sol-gel method was used to synthesize 0.1M IGZO (mole ratio 9:1:2 of Indium, Gallium, and Zinc) solution [28]. The stock solution was prepared by dissolving 5N purity metal precursors (225.5 mg of indium nitrate hydrate (In(NO3. $\times$H2O)), 21.4 mg of gallium nitrate hydrate (Ga(NO3. $\times$H2O)) and 31.4 mg zinc nitrate hydrate (Zn(NO3. $\times$ H2O))) from Sigma Aldrich in 10 mL of 2-methoxyethanol (99% Sigma Aldrich). The Additives, namely 100μL of acetylacetone (aq) (Sigma Aldrich, 99%) and 40μL of ammonium hydroxide (aq) (28.0% NH3 in water, Aldrich, 99.99%) were added in IGZO solutions. After stirring above mixture at 800 rpm for 24 hours at room temperature, the final solution was filtered 0.22 μm PTFE syringe filter.

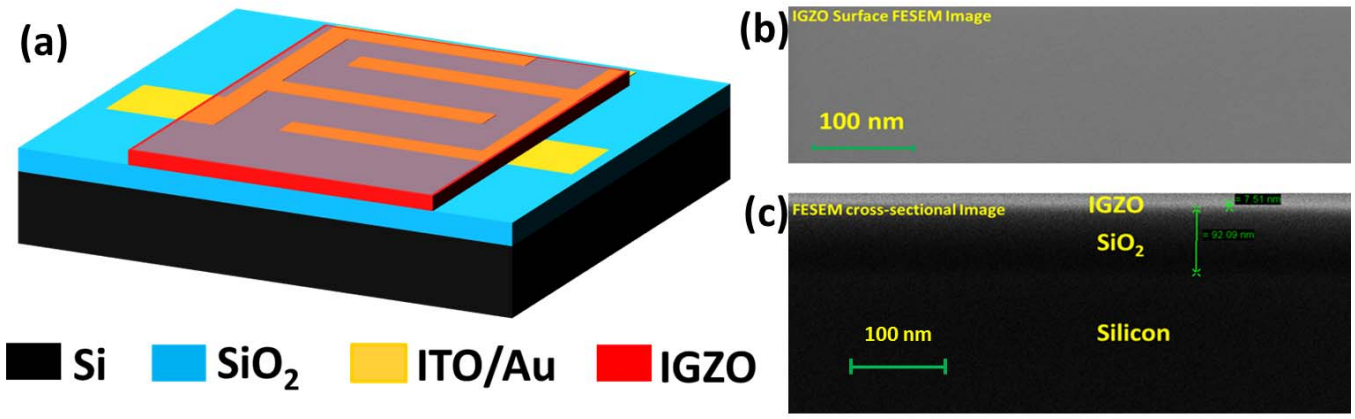

Fig. 1. (a) Schematic of the a-IGZO-TFT structure realized after fabrication in the cleanroom. The Width/length ratio of the a-IGZO-TFTs (W/L = 10000 μm / 20 μm). The gate oxide (SiO2) thickness is 100 nm. The spin-coated channel (IGZO) thickness is ~10nm. (b) IGZO Surface FESEM Image (c) FESEM Cross-sectional image of IGZO-TFT.

B. Fabrication of IGZO-TFTs

The bottom gate-bottom contact IGZO-TFTs were fabricated on highly doped silicon substrates (n++) from Fraunhofer IMPS. The substrate consisted an n-doped (doping: n $\approx 3 \times 10^{17}$ cm^{-3}) silicon $<100>$ wafer which acts as a gate, the thermally grown SiO_2 as the gate dielectric, and the interdigitated source/drain terminals ITO-gold patterned on SiO_2 (thickness = 100nm) to ensure large width to length (W/L = 10000μm/20μm) ratio. These substrates were ultrasonically cleaned in acetone and isopropyl alcohol (IPA) for 10 minutes each and dehydrated at 120 °C for 5 min to remove water traces. Further, UV ozone cleaning was done for 10 min to remove organic contaminants and improve the surface's wetting. Then, immediately the synthesized IGZO solution was spin-coated on the substrate at 3000 rpm for 30 Seconds under fume hood. The resulting thin layer of IGZO was annealed at 300 °C for 3 hours in the ambient air. A schematic illustration of the IGZO-TFT structure is shown in Fig. 1(a).The spin-coated a-IGZO thin-film was smooth surface (Fig. 1(b)) with thickness was around 8-10nm that was measured using a cross-sectional image (Fig. 1(c)) using Field Emission Scanning Electron Microscope (FESEM).

C. Gamma Irradiation

^{60}Co-Gamma-ray irradiation of a-IGZO-TFT was performed at room temperature using a Cobalt-60 γ-radiation source (Gamma Chamber (GC 5000), BRIT, India) at a dose rate of 16 Gy/min and dose range from 100 Gy to 10 kGy. During irradiation, no electrical bias was applied to the gate, drain and source terminals of the a-IGZO-TFT.

D. Microscopic and Electrical Characterization

The effects of γ-irradiation on different characteristics of the IGZO films and TFTs were investigated. X-Ray Diffraction (XRD) patterns of the pre and post γ-irradiated IGZO thin films were recorded using the Rigaku High-Resolution X-ray diffractometer with CuKα radiation (λ = 1.5418 A° and rated at 9 kW). Atomic force microscopy (AFM) imaging of the pre and post γ-irradiated IGZO surface was carried out with a 1μm^2 scan area using Asylum, MFP-3D conductive AFM system. The current-voltage (IV) characterization of the a-IGZO-TFT before and after irradiation was performed using Keithley 4200 Source-Measure Unit (SMU) under a dark inert atmosphere.

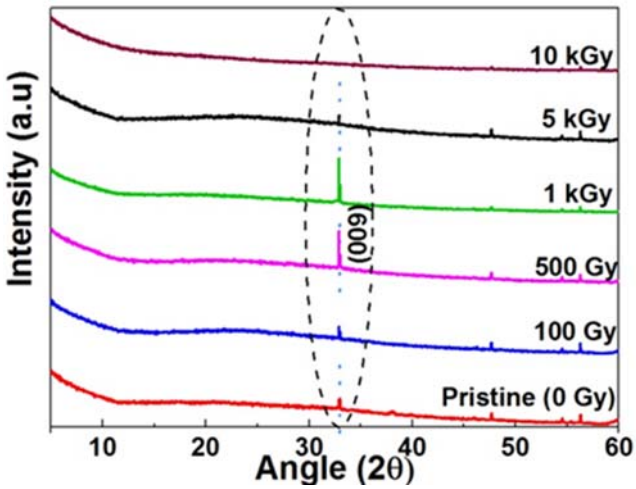

Fig. 2. XRD patterns of a-IGZO thin-film exposed to different doses of gamma radiation indicating the changes in (009) phase.

III. Results and Discussion

A. XRD of a-IGZO Thin-Film

The XRD patterns of the a-IGZO film before and after exposure to γ-radiation are shown in Fig. 2.

As can be seen a low intensity but a clear peak (009) of IGZO around 32° angle was observed in irradiated samples. The intensity of XRD peaks increased for lower radiation dose up to 1 kGy and later decreased with increasing radiation dose. Therefore, minor phase changes from amorphous to Nano-crystalline of the irradiated film were observed, which can be attributed to ionization of a-IGZO film by γ-irradiation [29]–[30].

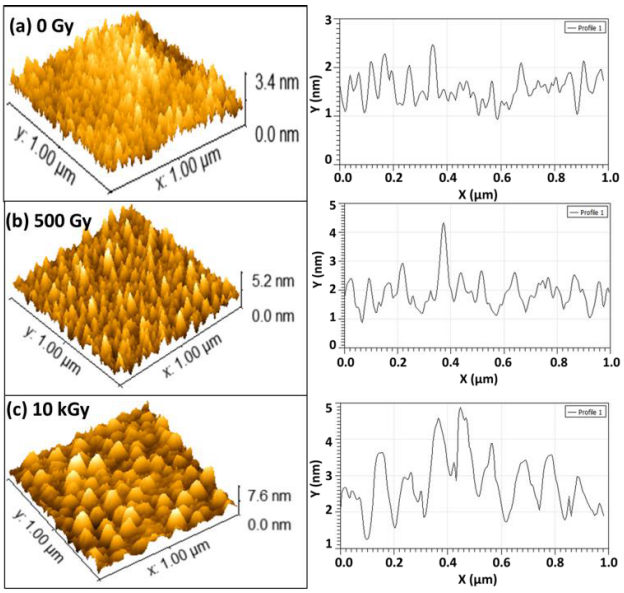

Fig. 3. AFM images of IGZO thin films of different γ-radiation doses (0 Gy, 500 Gy and 10 kGy). Image Scan Size is (1μm X 1μm) with corresponding roughness variation measurements.

B. Morphology Study of a-IGZO Thin-Film

The morphological variations and surface roughness of IGZO films exposed to γ-radiation were determined using an Atomic Force Microscopy (AFM). The RMS roughness was calculated using AFM software Gwyddion and presented for samples irradiated to different doses in Fig. 3. The RMS roughness value increases with increase in radiation dose. The RMS roughness observed was 0.2 nm, ~0.5 nm and ~1.5 nm for unirradiated, 500 Gy irradiated and 10 kGy irradiated samples, respectively. The increase of RMS roughness can be attributed to the radiation-induced surface reorganization. As clearly observed from AFM 3D images that large clusters were formed, this can be attributed to crystallites' agglomeration. In the oxide semiconductors, it is quite common that the grain size increases, and eventually, they agglomerate after gamma radiation. The AFM results are consistent with the findings of other researchers for the metal oxide thin-films [31]–[32].

C. Electrical Characterization Before Irradiation

The output and transfer characteristics of IGZO-TFTs before irradiation were measured at room temperature. Fig. 4(a) shows the corresponding output ($I_{ds}-V_{ds}$) characteristics for various gate bias steps. The lack of current crowding at low V_{ds} bias indicates good ohmic contact [33] and also, the device exhibits excellent gate control of the linear and saturation operation regimes of TFT. Fig. 4(b) shows the transfer characteristic ($I_{ds}-V_{gs}$) in semi-logarithmic and square root scales. The threshold voltage (V_{th}) was determined from a linear regression fit to the transfer characteristic $\sqrt{I_{ds}}-V_{gs}$ in the saturation region. The TFTs linear mode mobility (μ) was determined from (1) [24], [34].

$$\mu = \frac{\partial Ids}{\partial Vgs} \cdot \frac{L}{W \cdot Cox \cdot Vds} \tag{1}$$

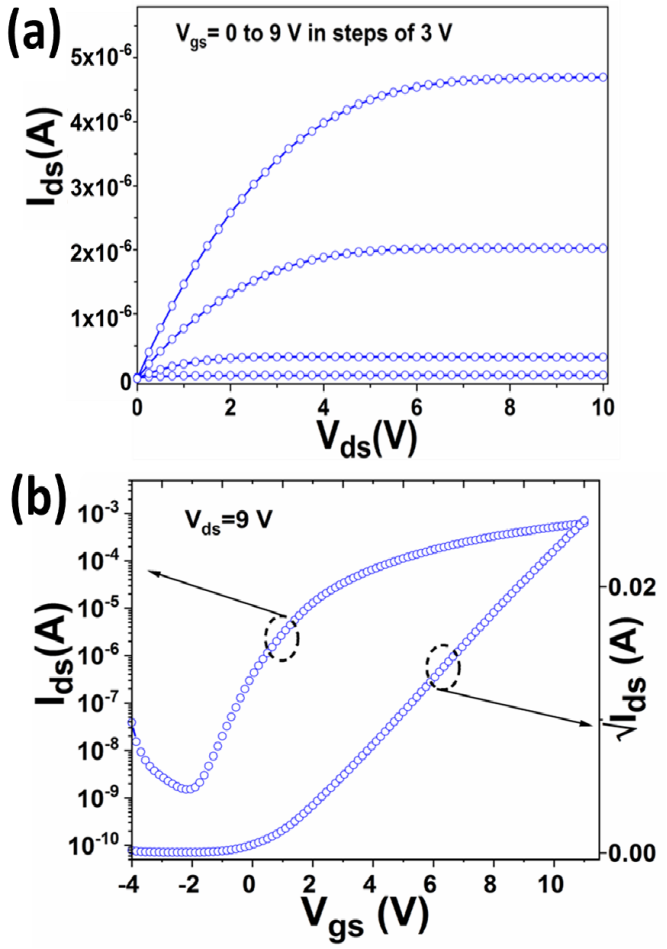

Fig. 4. (a) Output characteristics (I_{ds} versus V_{ds}) (b) Transfer Characteristics (log (I_{ds}) and $\sqrt{I_{ds}}$ versus V_{gs}) for IGZO-TFT before gamma irradiation. The Width/length ratio of TFTs (W/L = 10000 μm /20 μm). The gate oxide (SiO_2) thickness is 100 nm.

where C_{ox} is oxide capacitance, the mobility was determined using transfer characteristics for V_{ds} = 9V and V_{gs} =10V). The subthreshold swing (SS) is obtained from the slope of log (I_{ds}) versus V_{gs} that is (left curve in Fig. 4(b)). The solution-processed a-IGZO-TFTs exhibit excellent electrical characteristics.Total 40 TFTs were used in this study. The extracted parameters for the TFTs were in the range Vth= (0.5±0.3) V, μ = (0.85±0.25) cm2. V-1.s-1 and SS = (0.5 ± 0.3) V/decade. The TFTs showed minor hysteresis (0.3 ± 0.1) V in the transfer characteristics. The positive (+ 20V) and negative (-20 V) bias stress with source/drain terminals grounded was performed on TFTs. The positive shift of (0.3 ± 0.1 V) for positive bias stress and (0.2 ± 0.1 V) for negative bias stress was observed for bias stress for 1000 seconds. The interface trap density (N_{it}) at semiconductor/gate oxide interface is estimated from *SS* as in the equation in (2) [34],

$$N_{it} = \frac{Cox}{q}\left(\frac{q.SS.log\,(e)}{kT} - 1\right) \tag{2}$$

where q, k and T are the carrier charge, Boltzmann constant and working temperature, respectively. The maximum N_{it} is $\approx 1.1 \times 10^{12}$ cm^{-2}. eV^{-1} for the devices before irradiation.

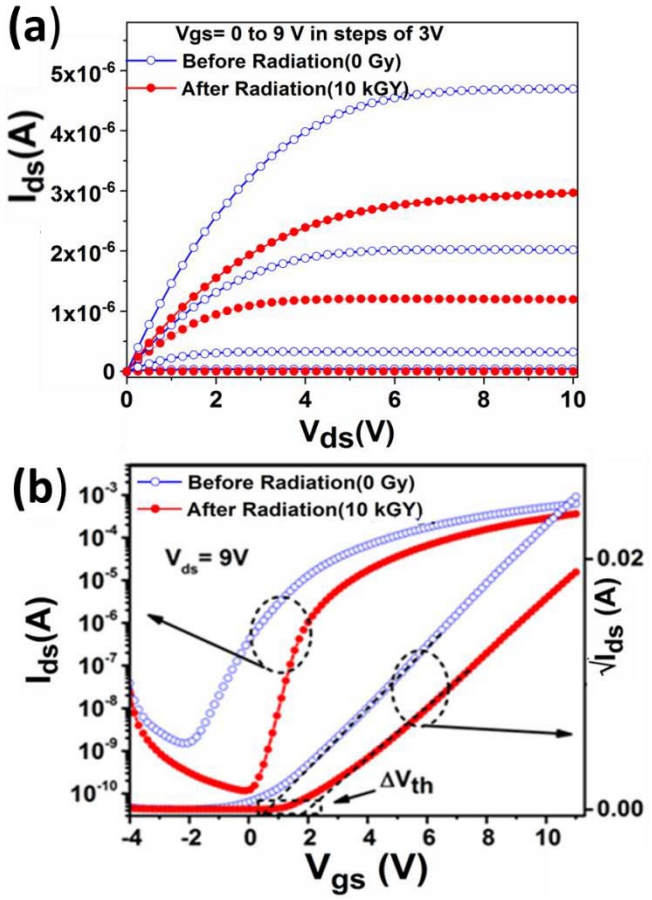

Fig. 5. (a) Output characteristics (I_{ds} versus V_{ds}) (b) Transfer Characteristics (log (I_{ds}) and $\sqrt{I_{ds}}$ versus V_{gs}) for IGZO-TFT with 10 kGy γ-radiation dose. The Width/length ratio of TFTs (W/L = 10000 μm /20 μm). The gate oxide (SiO2) thickness is 100 nm.

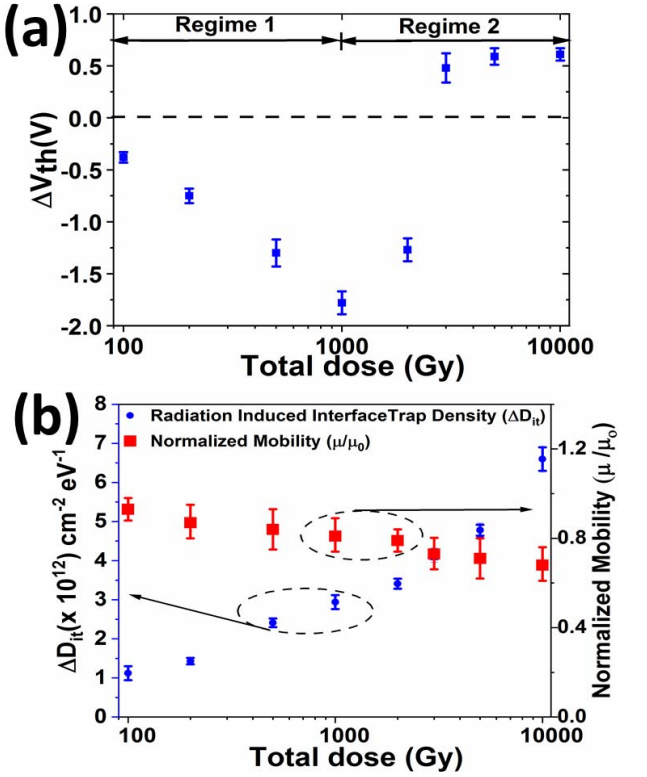

Fig. 6. (a) Threshold Voltage shift (b) Radiation-induced interface trap density (ΔD_{it}) and mobility change, as a function of the total dose. The Width/length ratio of TFTs (W/L = 10000 μm/20 μm). The gate oxide (SiO_2) thickness is 100 nm.

D. Radiation-Induced Effects in a-IGZO-TFTs

After completion of γ-irradiation, the electrical characteristics of TFTs were measured at room temperature. The performance parameters of the TFTs were extracted using similar procedure as described for TFTs before irradiation. The I-V characteristics were measured for a series of doses (100 Gy, 200 Gy, 500 Gy, 1 kGy, 2 kGy, 3 kGy, 5 kGy, and 10 kGy) and extracted TFT parameters. The output and transfer characteristics of a-IGZO-TFT with γ - radiation dose of 10 kGy are shown in Fig. 5 (a) and (b). It can be seen in Fig. 5(a), that there is a reduction in ON-current of TFTs. The positive V_{th} shift can be observed in Fig. 5(b). The threshold voltage shift (ΔV_{th}) is defined as the difference between the V_{th} of irradiated TFT and its pre-irradiated value. Fig. 6(a) shows Δ V_{th} as a function of the total dose that exhibits two distinct regimes. There is a negative shift of V_{th} with total radiation in the first regime (100 Gy to 1kGy). In the second regime (1kGy to 10kGy), a positive shift in V_{th} is observed. The two primary types of radiation-induced charges are oxide-trapped charge and interface-trap charge. In the TFTs with SiO2 as the gate dielectric, the threshold voltage initially shifted negatively upon irradiation. Positive oxide-trap charges are generated in a greater amount than the interface traps. The oxide-trap charges are acceptors for the upper half of the semiconductor's band-gap. With further irradiation, the interface traps' density begins to increase substantially and eventually greater than the radiation-induced oxide trap charges. As a result, the threshold voltage shifts back towards positive values. Thus, the change in the threshold voltage direction is apparently due to both radiation-induced charges. Interface traps and positive oxide charges are both generated and they compete with each other to influence the electrical performance of the TFTs [5], [35].

A curve fitting to the data ΔV_{th} versus radiation dose within the first regime (100 Gy to 1 kGy) and second regime (3 kGy to 10 kGy) was performed with the expression as indicated by (3). [36], [37].

$$\Delta V_{th} = A.D^n \tag{3}$$

where A is the radiation sensitivity of the device, n is the degree of linearity and D is the absorbed total dose. The fitting parameters obtained are A = 27.78mV$\pm$0.8mV/Gy, n = 0.73$\pm$0.04 (for 100 Gy to 1 kGy) and A = 14.38mV$\pm$ 0.1mV/Gy, n = 0.53$\pm$0.07 (for 3 kGy-10 kGy). Hence, the a-IGZO-TFTs can be used as radiation dosimeters for applications for radiation dose ranging from 100 Gy to 1 kGy.

The radiation-induced interface trap density (ΔD_{it}) can be determined as per the (4) [34]

$$\Delta D_{it} = (SS_{irradiated} - SS_0)\left(\frac{q}{kT.\ln(10)}\right)Cox \tag{4}$$

TABLE I
COMPARISON OF A-IGZO WITH REPORTED GAMMA RADIATION SENSORS

Ref	Transducer	Material	Parameter	Limit of detection	Sensitivity	Range (Gy)
[38]	MOS Capacitor	CuPc: Bi_2O_3	Threshold Voltage	50 Gy	8.3 mV/Gy	0- 500
[39]	MOS capacitors	Si/ Al_2O_3	Voltage to keep constant capacitance	1.5 kGy 2.9 kGy	20 μV/Gy 45 μV/Gy	0-8000
[36]	MOS Transistor	Si/ SiO_2	Threshold Voltage	2 Gy	20 mV/Gy	2-10
[40]	Resistor	TeO_2: In_2O_3	Conductivity	80 Gy	55 μGY/ μA/cm^2	0-100
[41]	RADFET (pMOS)	Si /SiO_2	Threshold Voltage	50 Gy	2.3 mV/Gy	0-200
[42]	POLY-Si TFT	Poly-Si/ SiO_2	Threshold Voltage	300 Gy	2.5 mV/Gy	300-1200
[43]	SOI-MOSFET	Si/ SiO_2	Threshold Voltage	300 Gy	12.5 mV/Gy	30-300
[this work]	AOS -RADFET	a-IGZO	Threshold Voltage Mobility	100 Gy	27.7±0.8 mV/Gy (100Gy-1kGy) 14.38 ±0.1 mV/Gy (3kGy-10kGy) $13x10^{-3}$ $cm^2.V^{-1}$-s^{-1}/Gy (100Gy-10kGy)	100-10000

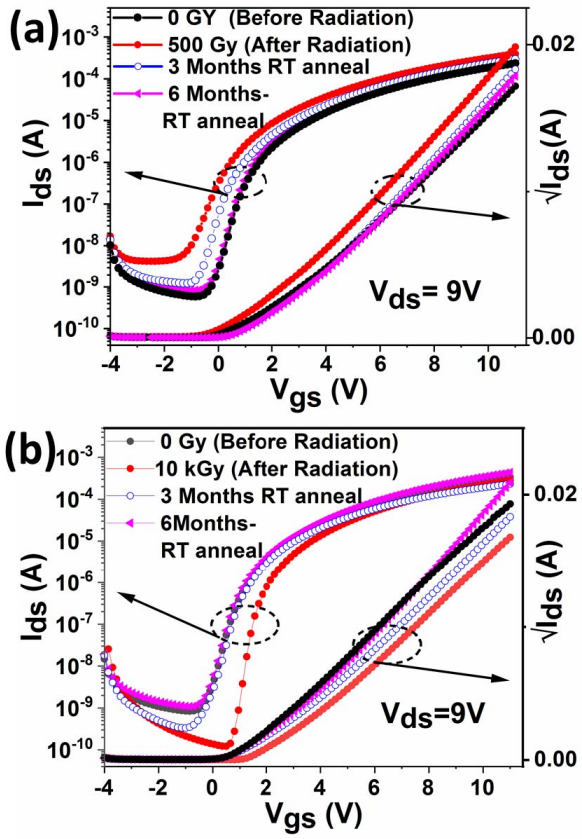

Fig. 7. (a) Transfer Characteristics (log (I_{ds}) and $\sqrt{I_{ds}}$ versus V_{gs}) of IGZO-TFTs before radiation, immediately after (a) 500 Gy irradiation (b) 10 kGy irradiation, and after room temperature annealing for three months and six months. The Width/length ratio of TFTs (W/L = 10000 μm/20 μm). The gate oxide (SiO_2) thickness is 100 nm.

where, SSirradiated is the subthreshold swing of a TFT after the desired radiation dose and SS0 is the un-irradiated threshold swing. As shown in Fig. 6(b), ΔDit is increasing monotonically. A plot of effective channel mobility (μ) normalized with respect to the pre-irradiated value (μo) is indicated in Fig. 6(b). The effective channel mobility is decreased slightly with radiation dose, where a total reduction of 23% for maximum radiation dose of 10 kGy. Here, the recovery behavior of V_{th} in conjunction with other parameters of the device helps create unique signatures to detect dose- levels, unlike other dosimeters [10], [36]. Further, a sensor array realized using IGZO-TFT and other dosimeters can help mitigate false positive alarms due to the generated unique signatures (feature set). Table. I details the comparison of a-IGZO-TFTs as a gamma radiation sensor with other reported sensors. Here, the devices such as metal oxide semiconductor (MOS) capacitors, MOS resistor, and TFTs with different channel/dielectric materials are considered to analyze the parameter variation with respect to radiation dose. The performance parameters considered for comparison are minimum radiation dose that can be detected (limit of detection) by a sensor, variation of sensing parameter with radiation dose (sensitivity), and range of radiation exposure. The a-IGZO-TFT sensor covers a wide range of radiation dose (100 Gy-10 kGy) with a limit of detection of 100 Gy. The sensitivity of the a-IGZO-TFT sensor is defined in terms of two parameters: mobility change ($\Delta\mu$/Gy) and threshold voltage shift (ΔVth/Gy) with radiation dose. The sensor exhibits sensitivity ($\Delta\mu$/Gy) of 13×10^{-3} $cm^2.V^{-1}.s^{-1}$/Gy for a wide range of 100 Gy to 10 kGy exposure. The sensor shows the highest sensitivity (ΔVth/Gy) of 27mV/Gy for a broader radiation dose of 100 Gy to 1 kGy. The sensitivity is 14.38 mV/Gy for radiation dose ranging from 3 kGy to 10 kGy.

E. Effect of Room Temperature Annealing

The γ-irradiated TFTs after electrical characterization were stored in vacuum at room temperature, defined here as room temperature (RT) annealing. The I-V characteristics of TFTs

TABLE II
SUMMARY OF TFT PARAMETERS AFTER RT ANNEALING

Parameter	Radiation dose 500 Gy		Radiation dose 10 kGy	
	AR[a]	RTA[b]	AR	RTA
ΔV_{th} (V)	- 0.92	-0.15	0.78	-0.10
ΔS (V/dec)	0.81	0.08	0.90	0.11
μ/μ_o	0.84	0.93	0.76	0.90
I_{ON}/I_{OFF}	$5x10^4$	$1x10^5$	$1x10^5$	$4x10^5$

[a] After Radiation [b] Room Temperature annealing (for 6 Month)

were measured at an interval of three months. Fig.7 (a) and (b) indicate the transfer characteristics of the RT-annealed TFTs [a] After Radiation [b] Room Temperature annealing (for 6 Month) exposed to γ-irradiation of 500 Gy and 10 kGy. The recovery of the TFT parameter after RT-annealing for 6 months is summarized in Table II. A gradual recovery of all γ-irradiated a-IGZO-TFT's intrinsic characteristics post room temperature storage in the vacuum for 6-months was observed.

IV. CONCLUSION

The gamma irradiation causes the threshold voltage to shift negatively for radiation dose up to 1 kGy and positively for radiation dose more than 1 kGy. The density of interface states increases from 1.1×10^{12} $cm^{-2}.eV^{-1}$ for un-irradiated TFT to 6.8×10^{12} $cm^{-2}.eV^{-1}$ for irradiated TFT with radiation dose of 10 kGy. The field-effect mobility decreases by 23% for a highest radiation dose of 10 kGy. The gamma irradiation has insignificant or no effect on the structure and morphology of a-IGZO film. The effect of gamma radiation on the TFTs' electrical characteristics is mainly due to the combined effects of the creation of interface states and gate oxide charges. The room temperature storage for a brief period of 6 months in vacuum showed gamma-irradiated TFTs' recovery. A-IGZO-TFT's reliability is found to be better than a-Si and a-IZO-TFTs in a harsh ionizing radiation environment. Moreover, this sensor device, when employed in a sensor array with other solution-processable materials, yield unique signatures. The advantage of low-cost fabrication and better radiation reliability of solution-processed a-IGZO-TFT makes it a potential candidate for applications in harsh radiation environments such as spacecraft, nuclear reactors, and medical radiation detectors.

DECLARATION OF COMPETING INTEREST

We declare that we have no financial and personal relationships with other people or organizations that can inappropriately influence our work; there is no professional or other personal interest of any nature or kind in any product.

ACKNOWLEDGMENT

This work was supported by Department of Science and Technology (DST), Government of India for project funding under the sanction letter No. SR/NM/TP-56/2016-IITB(G),and CEN, IITBNF-IIT-Bombay for the nanofabrication facility provided for device fabrication and characterization and AMS (ISOMED facility), RTDD, BARC, Mumbai for providing gamma radiation facility and Ms. Shubhangi A. Shelkar, AMS, RTDD, BARC for assisting in gamma irradiation of samples.

REFERENCES

[1] E. Fortunato, P. Barquinha, and R. Martins, "Oxide semiconductor thin-film transistors: A review of recent advances," *Adv. Mater.*, vol. 24, no. 22, pp. 2945–2986, 2014.
[2] P. Heremans *et al.*, "Mechanical and electronic properties of thin-film transistors on plastic, and their integration in flexible electronic applications," *Adv. Mater.*, vol. 28, no. 22, pp. 4266–4282, Jun. 2016.
[3] L. Zhou *et al.*, "High-performance flexible organic light-emitting diodes using embedded silver network transparent electrodes," *ACS Nano*, vol. 8, no. 12, pp. 12796–12805, Dec. 2014.
[4] M. Kaltenbrunner *et al.*, "An ultra-lightweight design for imperceptible plastic electronics," *Nature*, vol. 499, no. 7459, pp. 458–463, Jul. 2013.
[5] T. R. Oldham and F. B. McLean, "Total ionizing dose effects in MOS oxides and devices," *IEEE Trans. Nucl. Sci.*, vol. 50, no. 3, pp. 483–499, Jun. 2003.
[6] D. Fleetwood *et al.*, "Effects of oxide traps, interface traps, and border traps on metal-oxide-semiconductor devices," *J. Appl. Phys.*, vol. 73, no. 10, pp. 5058–5074, 1993.
[7] F. B. McLean and H. E. Boesch, "Time-dependent degradation of MOSFET channel mobility following pulsed irradiation," *IEEE Trans. Nucl. Sci.*, vol. 36, no. 6, pp. 1772–1783, Dec. 1989.
[8] L. L. Bras, M. Bendada, P. Mialhe, E. Blampain, and J. P. Charles, "Recombination via radiation-induced defects in field-effect transistor," *J. Appl. Phys.*, vol. 76, no. 10, pp. 5676–5680, 1994.
[9] T. R. Oldham, F. B. McLean, H. E. Boesch, and J. M. McGarrity, "An overview of radiation-induced interface traps in MOS structures," *Semicond. Sci. Technol.*, vol. 4, no. 12, pp. 986–999, Dec. 1989.
[10] S. Jain, S. Surya, P. Kumar, A. Gupta, and R. Rao, "Sensitivity improvement of medical dosimeters using solution processed TIPS-pentacene FETs," *IEEE Sensors J.*, vol. 19, no. 12, pp. 4424–4428, Jun. 2019.
[11] M. R. Shaneyfelt, P. E. Dodd, B. L. Draper, and R. S. Flores, "Challenges in hardening technologies using shallow-trench isolation," *IEEE Trans. Nucl. Sci.*, vol. 45, no. 6, pp. 2584–2592, Dec. 1998.
[12] H. L. Hughes and J. M. Benedetto, "Radiation effects and hardening of MOS technology: Devices and circuits," *IEEE Trans. Nucl. Sci.*, vol. 50, no. 3, pp. 500–521, Jun. 2003.
[13] N. Hastas, C. Dimitriadis, J. Brini, G. Kamarinos, V. Gueorguiev, and S. Kaschieva, "Effects of gamma-ray irradiation on polycrystalline silicon thin-film transistors," *Microelectron. Rel.*, Vol. 43, no. 1, pp. 57–60, 2003.
[14] E. H. Lee, A. Indluru, D. R. Allee, L. T. Clark, K. E. Holbert, and T. L. Alford, "Effects of gamma irradiation and electrical stress on a-Si: H thin-film transistors for flexible electronics and displays," *J. Display Technol.*, vol. 7, no. 6, pp. 325–329, Jun. 2011.
[15] M. Coll *et al.*, "Towards oxide electronics: A Roadmap," *Appl. Surf. Sci.*, vol. 482, pp. 1–93, Jul. 2019.
[16] T. Kamiya, K. Nomura, and H. Hosono, "Origins of high mobility and low operation voltage of amorphous oxide TFTs: Electronic structure, electron transport, defects and doping," *J. Display Technol.*, vol. 5, no. 7, pp. 273–288, Jul. 2009.
[17] T. Kamiya, K. Nomura, and H. Hosono, "Present status of amorphous In-Ga-Zn-O thin-film transistors," *Sci. Technol. Adv. Mater.*, vol. 11, no. 4, p. 23, Nov. 2010.
[18] P. K. Nayak *et al.*, "Zinc concentration dependence study of solution processed amorphous indium gallium zinc oxide thin film transistors using high-k dielectric," *Appl. Phys. Lett.*, vol. 97, no. 18, 2010, Art. no. 183504.
[19] A. Olziersky *et al.*, "Role of Ga_2O_3–In_2O_3–ZnO channel composition on the electrical performance of thin-film transistors," *Mater. Chem. Phys.*, vol. 131, nos. 1–2, pp. 512–518, Dec. 2011.
[20] K. Nomura, H. Ohta, A. Takagi, T. Kamiya, M. Hirano, and H. Hosono, "Room-temperature fabrication of transparent flexible thin-film transistors using amorphous oxide semiconductors," *Nature*, vol. 432, no. 7016, pp. 488–492, Nov. 2004.
[21] J. Troughton and D. Atkinson, "Amorphous InGaZnO and metal oxide semiconductor devices: An overview and current status," *J. Mater. Chem. C*, vol. 7, no. 40, pp. 12388–12414, 2019.
[22] J. Ramirez *et al.*, "Radiation-hard ZnO thin film transistors," *IEEE Trans. Nucl. Sci.*, vol. 62, no. 3, pp. 1399–1404, Jun. 2015.
[23] Y. Liu, W. Wu, Y. En, L. Wang, Z. Lei, and X. Wang, "Total dose ionizing radiation effects in the indium-zinc oxide thin-film transistors," *IEEE Electron Device Lett.*, vol. 35, no. 3, pp. 369–371, Mar. 2014.
[24] A. Indluru, K. E. Holbert, and T. L. Alford, "Gamma radiation effects on indium-zinc oxide thin-film transistors," *Thin Solid Films*, vol. 539, pp. 342–344, Jul. 2013.

[25] A. Koyama *et al.*, "Radiation stability of an InGaZnO thin-film transistor in heavy ion radiotherapy," *Biomed. Phys. Eng. Exp.*, vol. 3, no. 4, Jul. 2017, Art. no. 045009.
[26] T. Cramer *et al.*, "Radiation-tolerant flexible large-area electronics based on oxide semiconductors," *Adv. Electron. Mater.*, vol. 2, no. 7, Jul. 2016, Art. no. 1500489.
[27] R. A. Lujan and R. A. Street, "Flexible X-ray detector array fabricated with oxide thin-film transistors," *IEEE Electron Device Lett.*, vol. 33, no. 5, pp. 688–690, May 2012.
[28] C. Choi *et al.*, "Fabrication of high-performance, low-temperature solution processed amorphous indium oxide thin film transistors using a volatile nitrate precursor," *J. Mater. Chem. C*, vol. 3, no. 4, pp. 854–860, 2015.
[29] Y. Wang *et al.*, "Highly transparent solution processed In-Ga-Zn oxide thin films and thin film transistors," *J. Sol-Gel Sci. Technol.*, vol. 55, no. 3, pp. 322–327, Sep. 2010.
[30] Y.-H. Yang, S. S. Yang, C.-Y. Kao, and K.-S. Chou, "Chemical and electrical properties of low-temperature solution-processed In–Ga–Zn-O thin-film transistors," *IEEE Electron Device Lett.*, vol. 31, no. 4, pp. 329–331, Apr. 2010.
[31] K. Agashe *et al.*, "Effect of gamma irradiation on resistive switching of Al/TiO_2/n^+Si ReRAM," *Nucl. Instrum. Methods Phys. Res. B, Beam Interact. Mater. At.*, vol. 403, pp. 38–44, Jul. 2017.
[32] A. M. A. Ali *et al.*, "Effect of gamma irradiation dose on the structure and pH sensitivity of ITO thin films in extended gate field effect transistor," *Results Phys.*, vol. 12, pp. 615–622, Mar. 2019.
[33] K. Takechi, M. Nakata, T. Eguchi, H. Yamaguchi, and S. Kaneko, "Study on current crowding in the output characteristics of amorphous InGaZnO4Thin-film transistors using dual-gate structures with various active-layer thicknesses," *Jpn. J. Appl. Phys.*, vol. 48, no. 8, Aug. 2009, Art. no. 081606.
[34] D. K. Schroder, *Semiconductor Material and Device Characterization*, 2nd ed. New York, NY, USA: Wiley, 1998, pp. 500–504.
[35] K. K. Lee, D. Wang, O. Shinobu, and T. Ohshima, "Reliability of gamma-irradiated n-channel ZnO thin-film transistors: Electronic and interface properties," *Radiat. Effects Defects Solids*, vol. 173, nos. 3–4, pp. 250–260, Apr. 2018.
[36] G. Ristic, S. Golubovic, and M. Pejovic, "PMOS transistor for dosimetry application," *Electron. Lett.*, vol. 29, no. 18, pp. 1644–1646, Sep. 1993.
[37] S. Ashrafi and B. Eslami, "Investigation of sensitivity and threshold voltage shift of commercial MOSFETs in gamma irradiation," *Nucl. Sci. Techn.*, vol. 27, no. 6, p. 144, Dec. 2016.
[38] K. Arshak, A. Arshak, S. Zleetni, and O. Korostynska, "Thin and thick films of metal oxides and metal phthalocyanines as gamma radiation dosimeters," *IEEE Trans. Nucl. Sci.*, vol. 51, no. 5, pp. 2250–2255, Oct. 2004.
[39] L. S. Salomone *et al.*, "Radiation and bias switch-induced charge dynamics in Al_2O_3-based metal-oxide-semiconductor structures," *J. Appl. Phys.*, vol. 116, no. 17, Nov. 2014, Art. no. 174506.
[40] S. Sharma and T. Maity, "Effect of gamma radiation on electricl and optical properties of $(TeO_2)_{0.9}$ $(In_2O_3)_{0.1}$ thin films," *Bull. Mater. Sci.*, vol. 34, no. 1, pp. 61–69, Feb. 2011.
[41] G. S. Ristić, N. D. Vasović, M. Kovaćević, and A. B. Jakšić, "The sensitivity of 100nm RADFETs with zero gate bias up to dose of 230Gy(Si)," *Nucl. Instrum. Methods Phys. Res. Sect. B, Beam Interact. With Mater. At.*, vol. 269, no. 23, pp. 2703–2708, Dec. 2011.
[42] E. V. Jelenković *et al.*, "N-channel polysilicon thin film transistors as gamma-ray detectors," *Meas. Sci. Technol.*, vol. 24, no. 10, Oct. 2013, Art. no. 105103.
[43] M. R. Shaneyfelt *et al.*, "An embeddable SOI radiation sensor," *IEEE Trans. Nucl. Sci.*, vol. 56, no. 6, pp. 3372–3380, Dec. 2009.

Maruti B. Zalte received the B.Tech. degree from Dr. B.A.M. University, Aurangabad, India, in 1999, and the master's degree in electronics & telecommunication from the University of Pune, India, in 2001. Since 2001, he has been an Assistant Professor with the Department of Electronics & Telecommunication, K.J. Somaiya College of Engineering, Mumbai, India. He is currently pursuing the Ph.D. degree with the Department of Electrical Engineering, Indian Institute of Technology Bombay, Mumbai, under the quality improvement program (QIP). He is currently engaged in the project, where he is developing the low cost sensors using solution processable metal oxide semiconductor-based thin-film transistor platform for environmental monitoring and agricultural applications.

Virendra Kumar received the master's degree from IIT Roorkee and the Ph.D. degree from Mumbai University. He completed his two years postdoctoral research from ENSCP, Université Pierre et Marie Curie, Paris, France. He has been working on basic and applied aspects of radiation processing of polymeric materials for environmental, healthcare, and industrial applications. He is currently the Head of the Advanced Materials Section, RTDD, Bhabha Atomic Research Centre (BARC), and also an Associate Professor of HBNI, Mumbai. He has more than 210 publications including international journals, books, technical reports, and conference, and 40 invited talks to his credit. His research interests include polymer modification via radiation grafting process for applications, such as functional adsorbents for remediation of toxic water pollutants, antibacterial surface, recyclable catalytic systems, metal nanoparticle based optical sensors, radiation cured inorganic/organic nano-composites coating, anti-fouling, and super-hydrophobic polymer coatings by PECVD process. He has been actively involved in Board of Research in Nuclear Sciences (BRNS) and International Atomic Energy Agency (IAEA) activities in the field of radiation processing of polymers. He was a recipient of the DAE-Scientific & technical Excellence Award in 2016, the DAE-Group Achievement Award in 2016, the IANCAS-Dr. Tarun Dutta Memorial Award in 2016, and the ISRAPS-Dr. P. K. Bhattacharya Memorial Young Scientist Award in 2006.

Sandeep G. Surya (Member, IEEE) received the B.Tech. degree from JNTU, Hyderabad, in 2008 and the Ph.D. degree from IIT Bombay in 2017. He was a Postdoctoral Research Fellow with the King Abdullah University of Science and Technology (KAUST), Saudi Arabia. He is currently a Senior Research Scientist with Prognomics Ltd., Swansea, U.K. He was a Research Associate with the Microsystems Technology Research Unit, CMM, Fondazione Bruno Kessler (FBK), Trento, Italy. He has authored or coauthored 40 international journal and conference articles, the inventor/co-inventor of four U.S. and one Indian patent. He was a member of different teams working on explosive detectors and telemedicine. His work received the Gandhian Young Technological Innovation Award at IIM-A 2012, the Fellowship at ISED 2011, the Best Novelty Prize for a Humanoid Robot at IIIT-H and the P.P Chhabria Award of Excellence in intelligent systems and robotics for the year 2009 at IIIT, Pune.

Maryam Shojaei Baghini (Senior Member, IEEE) received the M.S. and Ph.D. degrees in electrical engineering from the Sharif University of Technology, Tehran, in 1991 and 1999, respectively. She worked in industry as a Senior Analog IC Designer followed by postdoctoral research with IIT Bombay, where she is currently a TATA Trust Chair Professor with the Department of Electrical Engineering. She has published more than 270 peer reviewed international journal and conference articles. She is the inventor/coinventor of six granted U.S. patents, five granted Indian patents, and 42 more filed patent applications. Her research interests include from devices and sensors to the integrated instrumentation circuits & sensor systems and analog/mixed-signal/RFdesign. She has served as in the technical program committee for several IEEE conferences including the WSN Track Chair in the IEEE Sensors Conference 2018 and 2019. Prof. Shojaei is a Fellow of INAE and recipient/joint recipient of 13 awards.